O. V. Belov[1,*], O. Chuluunbaatar[1,2,**],
M. I. Kapralov[1], N. H. Sweilam[3,***]

THE ROLE OF THE BACTERIAL MISMATCH
REPAIR SYSTEM IN SOS-INDUCED MUTAGENESIS:
A THEORETICAL BACKGROUND

[1] Joint Institute for Nuclear Research, Dubna
[2] National University of Mongolia, Ulaanbaatar
[3] Cairo University, Giza, Egypt
* E-mail: dem@jinr.ru
** E-mail: chuka@jinr.ru
*** E-mail: nsweilam@sci.cu.edu.eg

Белов О. В. и др.   E19-2012-96

Роль бактериальной системы репарации ошибочно спаренных

оснований в SOS-индуцированном мутагенезе:

теоретические аспекты

Выполнено теоретическое исследование роли репарации ошибочно спаренных осно-
ваний в реализации мутагенеза, индуцированного ультрафиолетовым излучением в бак-
териальных клетках *Escherichia coli*. Для этой цели разработана математическая модель
данного вида репарации, в рамках которой на основе современных экспериментальных
данных смоделированы ключевые пути реализации этого механизма. Детально описаны
пять основных путей удаления ошибок с участием разных ДНК-экзонуклеаз. При помощи
выполненных расчетов проверена гипотеза о том, что репарация неправильно спаренных
оснований отвечает за удаление нуклеотидов, ошибочно вставленных ДНК-полимеразой
V (комплексом $UmuD'_2C$) в ходе SOS-ответа, индуцированного ультрафиолетовым излу-
чением. Для анализа частоты мутаций предложенный модельный подход был совмещен
с разработанной ранее моделью индуцированного SOS-мутагенеза в клетках *E. coli*. Вы-
полненные расчеты подтвердили гипотезу о влиянии репарации ошибочно спаренных
оснований на мутаген при действии ультрафиолетового излучения.

Belov O. V. et al.   E19-2012-96

The Role of the Bacterial Mismatch Repair System

in SOS-Induced Mutagenesis: A Theoretical Background

A theoretical study is performed of the possible role of the methyl-directed mismatch
repair system in the ultraviolet-induced mutagenesis of *Escherichia coli* bacterial cells. For
this purpose, a mathematical model of the bacterial mismatch repair system is developed.
Within this model, the key pathways of this type of repair are simulated on the basis of
modern experimental data related to its mechanisms. Here we have modelled in detail five
main pathways of DNA misincorporation removal with different DNA exonucleases. Using
our calculations, we have tested the hypothesis that the bacterial mismatch repair system is
responsible for the removal of the nucleotides misincorporated by DNA polymerase V (the
$UmuD'_2C$ complex) during ultraviolet-induced SOS response. For the theoretical analysis of
the mutation frequency, we have combined the proposed mathematical approach with the model
of SOS-induced mutagenesis in the *E. coli* bacterial cell developed earlier. Our calculations
support the hypothesis that methyl-directed mismatch repair influences the mutagenic effect
of ultraviolet radiation.

1. INTRODUCTION

One of the biological systems capable of correcting the non-complementary nucleotide pairs that appear as a consequence of certain factors is the methyl-directed mismatch repair system (MMR) [1, 2]. Evidence of functioning of this system was found in many organisms, including bacteria, yeasts, and mammals. Despite high MMR conservability and the similarity of the repair mechanisms between bacteria and mammals, the interrelations between the pathways of these mechanisms and other repair systems are well understood only for relatively simple biological objects, like prokaryotic cells.

The factors which can start the MMR system may include the errors that occur during normal DNA replication and cell metabolism as well as a spectrum of DNA lesions induced by exposure to different agents of physical and chemical nature and subsequent DNA repair processes [3]. Among the physical factors capable of inducing this system, the action of radiations of different types is very interesting in terms of its use as an instrument for studying the MMR connections with other repair systems responsible for the mutagenic effects in the living organisms. There is a number of experimental facts supporting the possible role of MMR in the mutagenic effects of different types of radiations (mainly ionizing and ultraviolet) [4, 5]. Some of these facts suggest the involvement of MMR in mutagenic pathways of other repair systems.

Among the pathways leading to an increase in the mutation frequency and other negative effects under the influence of physical and chemical factors, an important role belongs to the SOS repair system [6–8]. Intensive studies of the SOS response of prokaryotic cells have identified the key role of the specific PolV Mut complex comprising DNA polymerase V (or UmuD$_2'$C) in the process of DNA synthesis through the lesion, which was called translesion synthesis [9]. This mechanism is realized not only in prokaryotic cells, but also in mammalian and human cells [10, 11].

Experimental studies have shown that PolV Mut demonstrates a relatively high error frequency during the incorporation of bases in nascent strands opposite the lesions, which were not removed during the earlier stages of repair [12]. However, the finally measured mutation frequency in individual genes is not so high as it might have been if all the errors produced by the PolV Mut complex had been fixed as mutations. Our previous research related to the mathematical modelling of the mechanism of SOS-induced mutagenesis under 254 nm ultraviolet (UV)

radiation demonstrated this fact by an interval of the free parameter value responsible for fixing the PolV-induced errors as mutations [13]. These conclusions made us introduce in our model additional repair mechanisms at the final stages of SOS response. Taking into account the specific character of DNA synthesis by the PolV Mut complex and relying on the corresponding experimental facts, we have chosen the MMR system of *E. coli* bacterial cells for the theoretical analysis of its influence on the UV-induced mutagenic effect. So the main goal of this study is to identify the role of MMR in SOS-induced mutagenesis on the basis of the precise modelling of the enzymatic mechanisms of these two repair systems under exposure to radiation.

2. THEORY

2.1. The Mechanism of MMR. Studies of the MMR system of bacterial cells have allowed us to find out the role of the main proteins in the regulation of the system's functions. The results of modern experiments as regards the description of the biochemical steps that follow MMR activation can be schematically summarized as it is shown in Fig. 1.
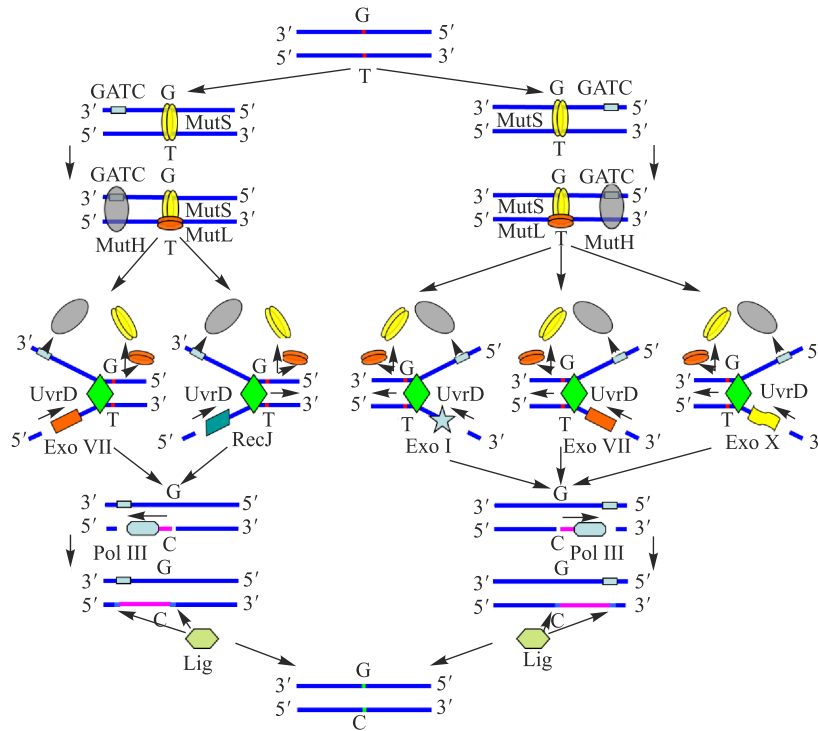

Fig. 1. Scheme of the MMR mechanism in *E. coli* bacterial cells (explanation in text)

After the occurrence of misincorporated nucleotides in the DNA chain, *E. coli's* MMR system detects the mismatch shortly after the DNA replication round ends. The way to detect an incorrect base on the newly synthetized strand is based on the process of DNA methylation, which does not occur until several minutes after the strand is produced. This mechanism provides a distinction between the parental strand, which is already methylated, and the daughter strand containing an error [1, 14]. The recognition of a wrongly incorporated nucleotide is performed by the MutS protein, which binds to the site with a mismatch as a homodimer and forms a complex with the MutL protein. Interaction with MutL enhances mismatch recognition, and recruits MutH protein to the region. In contrast with MutH, which acts as a monomer [3], MutL also functions as a homodimer. MutH finds a hemi-methylated dGATC sequence and joins the unmethylated DNA strand. Then the $MutS_2L_2$ complex activates the MutH protein in the presence of ATP. During this interaction, MutH makes a strand-specific nick that can occur either $3'$ or $5'$ to the mispair on the unmethylated strand. In the presence of MutL, helicase II (or UvrD) loads at the nicked site and unwinds the nascent strand [15]. The single-stranded DNA (ssDNA) produced in this process is bound by the single-strand binding protein (SSB), which protects ssDNA from a nuclease attack. Further MMR steps require the activity of four exonucleases: ExoI, ExoVII, ExoX, and RecJ encoded by the *xonA*, *xseA*, *exoX*, and *recJ* genes, respectively. These exonucleases are able to digest the nonmethylated strand from the dGATC nicked site to just beyond the mismatch. This excision process is bidirectional, i.e. exonucleases could proceed from $5'$ to $3'$ or from $3'$ to $5'$ end to the mispair [3]. ExoI and ExoX digest the DNA strand in the $3'$ to $5'$ direction, RecJ degrades it from $5'$ to $3'$, and ExoVII can excise DNA in both directions [16]. The resulting single-stranded gap is resynthesised by DNA polymerase III holoenzyme (PolIII) with SSB. The remaining DNA strand is joined to the existing one by the DNA ligase [2].

2.2. MMR and SOS Response. A number of experimental facts have recently allowed formulation of the hypothesis that the MMR system significantly reduces the error rates during DNA replication by recognizing and correcting mismatches, which prevent normal replication [17]. It was also found that MMR can process the incorrect bases opposite the UV-induced photoproducts, which were not removed by early repair processes, like photoreactivation, nucleotide excision repair or SOS response [4]. Summarizing all these facts, we can conclude that the main way of interaction between the inducible SOS system and MMR is the methyl-directed excision of incorrect bases inserted by PolV Mut in nascent strands during translesion synthesis. Under the induction of SOS response, the amount of the misincorporated bases, which are the substrate for MMR, becomes much higher than under normal conditions when MMR repairs mainly spontaneously induced lesions. Within our model approach, we show how

the interactions between these two systems could be realized taking into account the modern data on the biochemical mechanisms of the MMR and SOS systems.

3. MATHEMATICAL MODEL

In our previous study, we developed a mathematical model of the *E. coli's* mutation process induced by UV radiation [13, 18, 19]. Using this model, we analysed the chain of events from primary DNA lesion appearance to fixing this lesion as a mutation. We also described quantitatively the relationships between the biochemical processes realized during SOS response and the translesion synthesis effectiveness. It was shown how this model could be applied for the estimation of the mutagenic effect of UV radiation. We demonstrated this ability of our model by estimating the mutation frequency in *E. coli's lacI* gene. To describe the relationship between SOS response and MMR, we combine the model developed earlier with a newly designed mathematical approach to methyl-directed repair.

To design a model of MMR, we have simulated the dynamical changes of the concentrations of MMR proteins and intermediate complexes concentrations using reversible mass-action kinetics. The reaction network, which highlights mass transfer and regulatory reactions, is presented in Fig. 2.
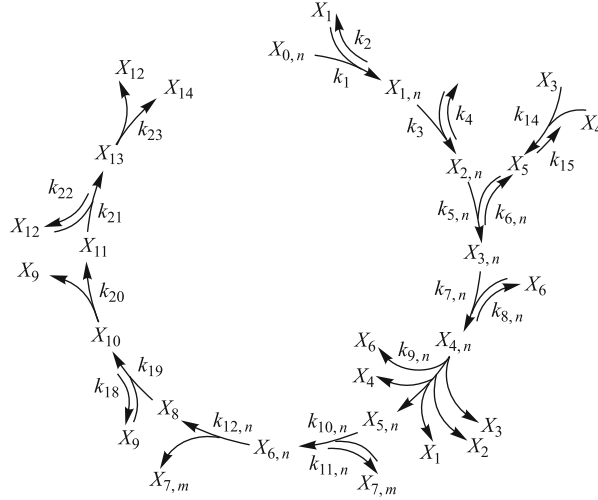

Fig. 2. Scheme representing the MMR reaction network used in the model. Here $X_{0,n}$, X_1, X_2, X_3, X_4, X_6, $X_{7,m}$, X_9, X_{12}, and X_{14} are the concentrations of mismatches, MutS$_2$, MutL$_2$, MutH, GATCm, UvrD, exonucleases of the m type, PolIII, DNA ligase, and repaired DNA, respectively; $X_{1,n}$, $X_{2,n}$, $X_{3,n}$, $X_{4,n}$, $X_{5,n}$, $X_{6,n}$, X_8, X_{10}, X_{11}, and X_{13} are the intermediates that are being formed during repair. Synthesis and nonspecific losses of the MMR proteins are omitted

4

In the general view, the equations of the model could be expressed as follows:

$$\frac{dX_i}{dt} = V_{i+}(X_i, X_0) - V_{i-}(X_i, X_0), \tag{1}$$

where X_i $(i = 1, \ldots, n)$ is the i-th regulatory protein intracellular concentration, X_0 is an inducing signal, which represents the amount of the nucleotides misincorporated by the PolV Mut complex, and t is time. The functions V_{i+} and V_{i-} describe the i-th protein accumulation and degradation, respectively.

For our model, we singled out five MMR pathways with four exonucleases taking into account their ability to digest a nascent DNA strand in different polarity. The dimensionless equations for each protein and intermediate complexes of the MMR system as well as their initial conditions are given in Appendix A (Eqs. (A.1)) in a concise form. We divided the total yield of errors produced by the PolV Mut complex into five subyields $X_{00,n}$ $(n = 1, \ldots, 5)$, which possess the corresponding $3'$ or $5'$ polarity depending on the position of the MutH-mediated nick and, therefore, should be repaired with different exonucleases. $X_{00,1}$ represents the mispairs with a $3'$ nick to their position to be repaired by the ExoI pathway; $X_{00,2}$ and $X_{00,3}$ are the subyields with $3'$ and $5'$ nicks to the mismatch, respectively, to be processed with ExoVII; $X_{00,4}$ and $X_{00,5}$ represent the yields with $3'$ and $5'$ nicks to be repaired by ExoX and RecJ pathways, respectively. In this study, we assume that $3'$ and $5'$ MutH-mediated nicks as well as the involvement of exonucleases possessing the same end specificity are equally probable.

Most genes encoding the main MMR proteins in *E. coli* cells are SOS-independent, i.e. their synthesis is not controlled by the LexA protein. However, the expression of the *uvrD* gene producing helicase II strongly depends on the intracellular concentration of the LexA repressor [20, 21]. To describe the regulation of the *uvrD* transcription by the LexA protein, we applied the model of gene regulation used in many papers [13, 22, 23]. The first term in the equation for the UvrD helicase (Eqs. (A.1)) describes the LexA-regulated synthesis. The dimensional expression for the UvrD protein synthesis is the following:

$$V_{6,\text{sint}} = \frac{kX_{06}\left(1 + \left(\frac{X_{0L}}{\gamma}\right)^h\right)}{1 + \left(\frac{X_L}{\gamma}\right)^h}. \tag{2}$$

Here X_{06} and X_{0L} are the dimensional initial concentrations of the UvrD helicase and the LexA protein, γ is the dissociation rate constant of the LexA monomer from the *uvrD* gene operator, h is the Hill coefficient characterizing the LexA binding cooperativity, X_L is the current intracellular LexA concentration, and k is the kinetic rate constant.

The values of the kinetic rate constants are defined using values measured experimentally and by fitting the model to existing experimental data on the MMR kinetics at different stages of repair. A complete set of model parameters and their normalization is provided in Appendix B.

To calculate $X_{00,1}$, $X_{00,2}$, $X_{00,3}$, $X_{00,4}$, and $X_{00,5}$, we used our translesion synthesis model developed earlier [13]. It describes DNA resynthesis at single strand gaps opposite thymine dimers by the PolV Mut complex and allows us to calculate the mean value of the errors produced by this complex depending on time and energy fluence of UV radiation. The input data for this model is the kinetics of the UmuD$_2'$C complex calculated in our previous study for UV energy fluences up to 100 J/m^2. In our model, $X_{00,1}$, $X_{00,2}$, $X_{00,3}$, $X_{00,4}$, and $X_{00,5}$ are directly proportional to the previously calculated average number of errors. Taking into account the equiprobability of launching all the five subpathways, we set these subyields equal to 1/5 of the error value.

Our model allows the description of the mutation process in individual genes. The dependence of the mutation frequency on the UV energy fluence is described by the following expression [8, 13]:

$$Z_m/Z(\Psi) = \theta_1\Psi + \theta_2\Psi(1 - \exp{(-\theta_3\Psi)}), \qquad (3)$$

where Z_m and Z are the numbers of the mutants and survived cells, respectively; Ψ is the UV energy fluence; $\theta_1\Psi$ is the linear component of the dependence; $\theta_2\Psi$ is proportional to the mutation yield, and $(1 - \exp{(-\theta_3\Psi)})$ is the share of cells in which the mutagenic repair has been induced.

In this paper, we have estimated the mutation frequency not only for the bacterial strains with the normal functioning of the MMR and SOS systems (mut^+ and umu^+ bacteria), but also for the mutant strains carrying defects in the *mutS*, *mutL*, *mutH* (mut^-), and *umuC* genes (umu^-). As a rule, the mut^- bacteria demonstrate a spontaneous level of mutagenesis. Therefore, in order to describe the mutation frequency in these strains, we need to introduce, in Eq. (3), a parameter θ_0, characterizing spontaneous mutagenesis:

$$Z_m/Z(\Psi) = \theta_0 + \theta_1\Psi + \theta_2\Psi(1 - \exp{(-\theta_3\Psi)}). \qquad (4)$$

This parameter, which is an input parameter of the model, does not depend on the UV energy fluence and can be specified on the basis of the experimental data. For the strains with the normal genotype, $\theta_0 = 0$ because the mutation frequency for these strains is negligible without irradiation [4]. The experimental values of θ_0 and θ_1 as well as the procedure of evaluating the parameters θ_2 and θ_3 are given in Appendix B.

For the umu^- bacteria, which are defective in SOS repair, we need to set $\theta_3 = 0$ because the share of cells with the induced SOS response will be zero. Therefore, the mutation frequency will depend only on spontaneous mutagenesis

6

and on the linear component characterizing the mutagenic lesions that are fixed either during the constitutive repair or DNA replication.

4. RESULTS

The results of the parameter-fitting procedure show an adequate set of parameters for the developed model (Figs. 3–5). The calculated curves reconstruct the kinetics of different *in vitro* MMR stages well. This fact enables us to use our model for the identification of intracellular mechanisms realizing the connections between the mutagenic SOS response and the methyl-directed mismatch repair. The developed model allows for a comprehensive quantitative analysis of protein–protein interactions within the molecular networks of these two systems. We do not show here the detailed data calculated for the dynamical change of MMR protein concentrations because the main purpose of this paper is to demonstrate the effect of the mismatch repair on the radiation-induced SOS mutagenesis.

Fig. 3. Incision of a $3'$ (●) and $5'$ (■) hemimethylated heteroduplexes by activated MutH in the presence of MutS and MutL. N is the concentration of incised DNA. The curves are the calculated results; the dots are the experimental data [27]
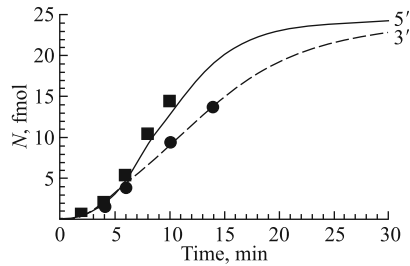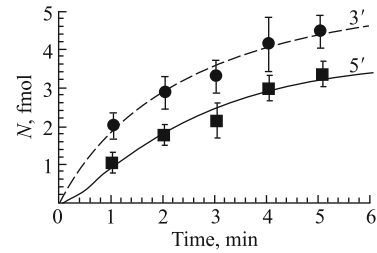

Fig. 4. Excision of a nicked $3'$ (●) and $5'$ (■) heteroduplexes by activated ExoI ($3'$) and RecJ ($5'$) in the presence of MutS, MutL, DNA helicase II, and SSB. N is the concentration of excised DNA. The curves are the calculated results; the dots are the experimental data [27]
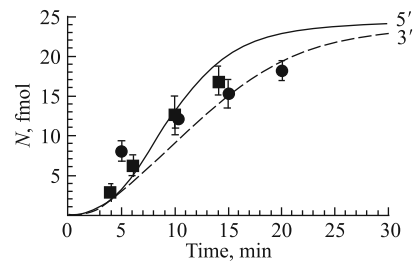

Fig. 5. DNA resynthesis of an excised $3'$ (●) and $5'$ (■) heteroduplexes by PolIII in the presence of MutS, MutL, DNA helicase II, ExoI or RecJ, and SSB. N is the concentration of rebuilt DNA. The curves are the calculated results; the dots are the experimental data [27]

7

4.1. Mutagenesis in Bacteria Defective in MMR Functions. Using our model, we have performed calculations of the mutation frequency in *E. coli* strains with different genotypes. The mutagenic effect of UV radiation was modelled for cells with normal SOS and MMR functions and for the three types of mutants defective in the *mutS*, *mutL*, or *mutH* gene. In this study, we have estimated the mutation frequency in the *E. coli's lacZ* gene encoding β-galactosidase. The computation procedure consisted in running simultaneously the models for SOS-induced mutagenesis, translesion synthesis, and the MMR system with the corresponding set of parameters responsible for the inhibition of MutS, MutL, or MutH protein functions (i.e. the parameters X_{01}, X_{02}, or X_{03} were assumed to be zero). Fig. 6 shows the results calculated for the mut^+ and $mutS^-$ strains in comparison with the experimental data on the revertant frequency in two alleles at *lacZ* codon 461, which reverts via CCC → C**T**C and C**T**T → C**T**C transitions [4]. We assume that these measured data reflect the general pattern of the mutagenic response of *E. coli* cells to UV radiation. In our calculations, we have obtained a 2.6-fold increase in the mutation frequency in a $mutS^-$ strain as compared with a mut^+ one. This value is the same as in the experiment mentioned above. At $\Psi = 0$ J/m^2, the curve computed for the $mutS^-$ strain starts from the average spontaneous level of mutagenesis equalling to $4 \cdot 10^{-8}$. For these two cases, our calculations give the following values of the parameter $P(X)$: $6.1 \cdot 10^{-8}$ for mut^+ and $1.6 \cdot 10^{-7}$ for $mutS^-$. The consideration of the MMR mechanism introduced into the model description of SOS-induced mutagenesis slightly changes the sense of this parameter. We indicated before that this parameter reflects the error probability during nucleotide pasting by PolV Mut on DNA sites, which do not contain thymine dimers. However, a more detailed understanding of the mechanisms behind $P(X)$ provides a new explanation of its meaning. It could be interpreted as the resulting probability of the error fixation after DNA resynthesis by the PolV Mut complex. It means that $P(X)$ reflects not only the error induction by PolV Mut, but also the probability of mutation appearance at the place of a wrongly inserted nucleotide. That is the main reason why the new values
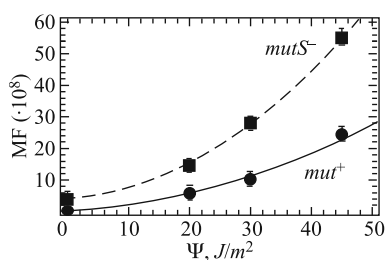

Fig. 6. Dependence of the mutation frequency on UV energy fluence calculated for mut^+ (the solid line) and $mutS^-$ (the dashed line) strains. The symbols represent experimental data for mut^+ (●) and $mutS^-$ (■) strains [4]. The experimental data with their standard errors of the means $(\cdot10^{-8})$ for mut^+ and $mutS^-$ are, respectively, 0 J/m^2, 0, 4.0 ± 0.4; 20 J/m^2, 14.4 ± 0.9, 5.7 ± 0.2; 30 J/m^2, 28.0 ± 3.4, 10.2 ± 0.9; 45 J/m^2, 55.0 ± 1.0, 24.4 ± 4.2

8

of this parameter are much lower than the ones obtained before [13]. Another fact that stipulates the lower $P(X)$ values is that the average error rate of PolV during the replication of undamaged DNA is $\sim 10^{-4}$ [24], but the resulting mutation frequency is much lower than it could have been if all the ssDNA gaps had been filled by this polymerase without any mechanism reducing its mutagenic activity.
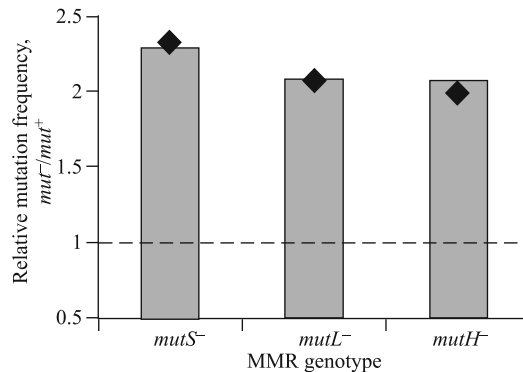

Fig. 7. Mutation frequency in bacteria defective in the *mutL* and *mutH* functions at the UV energy fluence of 30 J/m^2

We have also calculated the mutation frequency for $mutL^-$ and $mutH^-$ bacteria at a single UV energy fluence of 30 J/m^2 (Fig. 7). The obtained results for these strains are about two times higher than for the mut^+ ones, just like in the experiment [4]. The $P(X)$ parameter values for these cases are given in Appendix B. Taking into account the experimental standard errors of means (SEM), we can conclude that the model adequately reconstructs the observed mutagenic effect.

4.2. Mutagenesis in Bacteria Defective in SOS and MMR Functions. As is known, a defect in some of the *umuDC* genes leads to the inactivation of the SOS function because it prevents the normal assembling of the UmuD$_2'$C complex, which is the main component of PolV Mut. In our model, we reconstructed the mutagenic effect observed experimentally under the defect in *umuC* gene and violations in the *mutS*, *mutL*, and *mutH* functions of MMR systems. Setting the parameter θ_0 according to the average spontaneous mutation frequency for the $umu^- mut^-$ strains, we calculated the level of mutagenesis, which is equal to $\sim 5.7 \cdot 10^{-8}$ and is in line with the experimental data [4]. As for $umu^+ mut^-$ bacteria, the computation procedure included running three models together with the initial conditions reflecting the corresponding genotype, i.e. X_{01}, X_{02}, X_{03}, and the initial concentration of UmuC in the SOS-mutagenesis model were set to zero.

9

5. DISCUSSION

The results of our computations confirmed by the experimental data strongly accentuate the role of the MMR system in radiation-induced SOS mutagenesis. Choosing UV radiation as a mutagenic factor for this study is explained by the necessity to indicate the links between the MMR and SOS response without any significant influence of other repair systems such as single- and double-strand break repair and base excision repair. Since most of the UV-induced lesions represent, in dark conditions (photoreactivation is lacking), a substrate for both nucleotide excision repair and SOS repair, the interrelation between the biochemical mechanisms, MMR and SOS system can be identified more precisely. The developed models provide a topological view of the MMR and SOS networks, which is another way to clarify their biological relations. The precise modelling of enzymatic mechanisms together with the mathematical description of mutagenic effects bring a specific insight into the problem of induced mutagenesis, opening up a possibility of exploring the effects of different molecular mechanisms on the final mutagenic reaction of the living organism. In this paper, we have shown how more or fewer functions connected with the activity of the *mutS*, *mutL*, *mutH*, and *umuC* genes affect the mutation frequency, i.e. what influence the system's different topologies have on the final cell response to irradiation. It has been theoretically proven that the violation of the expression of one of these genes leads to an increase in bacteria mutagenesis. It is clear that this fact could be extrapolated to other SOS genes responsible for assembling the PolV Mut complex. According to our model, violations in the *umuD* or *recA* gene result in the same mutation frequency as in the *umuC*-defective strains.

Apart from our previous studies, only a few papers are concerned with simulating some quantitative characteristics of TLS [25, 26]. However, these approaches neither provide a systemic view of the process nor focus on its probabilistic aspects and connections with other repair systems. One of the main features of our models is a clear representation of cause-and-effect relations between two complicate repair networks and the TLS effectiveness. In addition to the quantitative analysis of mutagenic effects, the developed models provide a tool for the detailed analysis of the protein–protein interaction dynamics and a feedback between SOS response and MMR. We have not paid much attention to this issue in this paper.

Considering our models, one might think that the quantitative estimation of the mutagenic effects can be done with a much simpler analysis than the development of a complicated mathematical model for the computation of parameters in the classical equation for the mutation frequency. However, such a simplified approach gives no information as to which biophysical processes are behind these parameters. The models similar to ours clearly indicate the dependence of para-

meter values on real biological mechanisms. This justifies the claim to novelty and makes these models useful.

Taking into account the knowledge of the molecular mechanisms of other *E. coli's* repair systems, it could be suggested that the MMR system plays a role in SOS mutagenesis induced not only by UV radiation, but also by the ionizing radiations of different quality. The latter relates mostly to the repair of clustered DNA lesions, which are being formed after irradiation by charged particles, because it is assumed that these lesions make up the main substrate for the mutagenic SOS repair.

APPENDIX A. THE SYSTEM OF EQUATIONS

Eqs. (A.1) represent a concise form of the system of ordinary differential equations describing the MMR pathways. Here, $y_{0,n}$ are the normalized intracellular concentrations of the mismatches (Mism_n) produced by the PolV Mut complex, which will be repaired by n different pathways. The variable y_1 is the concentration of the MutS dimer, which recognizes a mismatch and binds to it reversibly, forming an intermediate $\text{Mism}_n\text{MutS}_2$ complex ($y_{1,n}$); y_2 represents the normalized concentration of the MutL dimer, which joins the $\text{Mism}_n\text{MutS}_2$ complex and forms the next intermediate $\text{Mism}_n\text{MutS}_2\text{MutL}_2$ ($y_{2,n}$). The variable y_3 is the concentration of the MutH protein interacting with the methylated GATCm sequence (y_4), yielding the GATCmMutH complex (y_5). The variables $y_{3,n}$ are the concentrations of the nicked DNA after the interaction of $\text{Mism}_n\text{MutS}_2\text{MutL}_2$ complexes with GATCmMutH. The molecules of the MutS_2, MutL_2, and MutH proteins remain joined to the nicked DNA strand. The following strand unwinding by the UvrD-helicase (y_6) can be represented as a typical enzymatic reaction with the intermediate complex $y_{4,n}$ and the resulting detachment of MutS_2, MutL_2, MutH, and UvrD.

Since the synthesis of the UvrD helicase is SOS-dependent, we introduced the normalized concentration of the LexA protein (y_L) into the equation for y_6. The kinetics of LexA is calculated using the model of SOS-induced mutagenesis [13]. The action of UvrD leads to the formation of an unwound DNA site $y_{5,n}$, which will be processed by five pathways with four exonucleases $y_{7,m}$ ($m = 1, \ldots, 4$ for ExoI, ExoVII, ExoX, and RecJ, respectively). The first pathway ($n = 1$) is related to the $3'$-nicked DNA excision by ExoI; the second and third ones ($n = 2$ and $n = 3$) describe the $3'$- and $5'$-nicked strand excision by ExoVII, respectively. When $n = 4$, the $3'$-nicked strand is cut out by ExoX, and for $n = 5$, the $5'$-nicked DNA excision is processed by RecJ. In our model, these interactions are also presented as enzymatic reactions with intermediate complexes between a nicked strand and the corresponding exonuclease ($y_{6,n}$), and the formation of a single-strand DNA gap (y_8). The variable

y_9 is the normalized concentration of PolIII, and y_{10} describes the amount of the intermediate complex representing PolIII molecules bound to a single-strand gap during DNA resynthesis. The variable y_{11} is the concentration of the newly synthesized DNA sequence with two small gaps at its edges. The last MMR stage is characterized in the model by a reaction describing the ligation of a new sequence by a DNA ligase (y_{12}), where y_{13} is the intermediate complex, and y_{14} is the repaired DNA.

$$\frac{dy_{0,n}}{d\tau} = p_2 y_{1,n} - p_1 y_1 y_{0,n},$$

$$\frac{dy_{1,n}}{d\tau} = p_1 y_1 y_{0,n} + p_4 y_{2,n} - y_{1,n}(p_2 + p_3 y_2),$$

$$\frac{dy_{2,n}}{d\tau} = p_3 y_2 y_{1,n} + p_{6,n} y_{3,n} - y_{2,n}(p_4 + p_{5,n} y_5),$$

$$\frac{dy_{3,n}}{d\tau} = p_{5,n} y_5 y_{2,n} + p_{8,n} y_{4,n} - y_{3,n}(p_{6,n} + p_{7,n} y_6),$$

$$\frac{dy_{4,n}}{d\tau} = p_{7,n} y_6 y_{3,n} - y_{4,n}(p_{8,n} + p_{9,n}),$$

$$\frac{dy_{5,n}}{d\tau} = p_{9,n} y_{4,n} + p_{11,n} y_{6,n} - p_{10,n} y_{7,m} y_{5,n},$$

$$\frac{dy_{6,n}}{d\tau} = p_{10,n} y_{7,m} y_{5,n} - y_{6,n}(p_{11,n} + p_{12,n}),$$

$$\frac{dy_1}{d\tau} = y_{01} + p_2 \sum_{n=1}^{5} y_{1,n} + \sum_{n=1}^{5} p_{9,n} y_{4,n} - y_1 \left(p_1 \sum_{n=1}^{5} y_{0,n} + p_{13} \right),$$

$$\frac{dy_2}{d\tau} = y_{02} + p_4 \sum_{n=1}^{5} y_{2,n} + \sum_{n=1}^{5} p_{9,n} y_{4,n} - y_2 \left(p_3 \sum_{n=1}^{5} y_{1,n} + p_{13} \right),$$

$$\frac{dy_3}{d\tau} = y_{03} + \sum_{n=1}^{5} p_{9,n} y_{4,n} + p_{15} y_5 - y_3(p_{14} y_4 + p_{13}),$$

$$\frac{dy_4}{d\tau} = y_{04} + \sum_{n=1}^{5} p_{9,n} y_{4,n} + p_{15} y_5 - y_4(p_{14} y_3 y_4 + p_{13}),$$

$$\frac{dy_5}{d\tau} = p_{14} y_3 y_4 + \sum_{n=1}^{5} p_{6,n} y_{3,n} - y_5 \left(\sum_{n=1}^{5} p_{5,n} y_{2,n} + p_{15} \right), \tag{A.1}$$

$$\frac{dy_6}{d\tau} = \frac{y_{06}(1 + p_{16})^h}{1 + (p_{17} y_L)^h} + \sum_{n=1}^{5} p_{8,n} y_{4,n} + \sum_{n=1}^{5} p_{9,n} y_{4,n} - y_6 \left(\sum_{n=1}^{5} p_{7,n} y_{3,n} + p_{13} \right),$$

$$\frac{dy_{7,1}}{d\tau} = y_{07,1} + y_{6,1}(p_{11,1} + p_{12,1}) - y_{7,1}(p_{10,1}y_{5,1} + p_{13}),$$

$$\frac{dy_{7,2}}{d\tau} = y_{07,2} + p_{12,1}y_{6,1} - y_{7,2}(p_{10,2}y_{5,2} + p_{10,3}y_{5,3} + p_{13}),$$

$$\frac{dy_{7,3}}{d\tau} = y_{07,3} + y_{6,4}(p_{11,4} + p_{12,4}) - y_{7,3}(p_{10,4}y_{5,4} + p_{13}),$$

$$\frac{dy_{7,4}}{d\tau} = y_{07,4} + y_{6,5}(p_{11,5} + p_{12,5}) - y_{7,4}(p_{10,5}y_{5,5} + p_{13}),$$

$$\frac{dy_8}{d\tau} = p_{18}y_{10} + \sum_{n=1}^{5} p_{12,n}y_{6,n} - p_{19}y_8y_9,$$

$$\frac{dy_9}{d\tau} = y_{09} + y_{10}(p_{18} + p_{20}) - y_9(p_{19}y_8 + p_{13}),$$

$$\frac{dy_{10}}{d\tau} = p_{19}y_8y_9 - y_{10}(p_{18} + p_{20}),$$

$$\frac{dy_{11}}{d\tau} = p_{20}y_{10} + p_{22}y_{13} - p_{21}y_{11}y_{12},$$

$$\frac{dy_{12}}{d\tau} = y_{012} + y_{13}(p_{22} + p_{23}) - y_{12}(p_{21}y_{11} + p_{13}),$$

$$\frac{dy_{13}}{d\tau} = p_{21}y_{11}y_{12} - y_{13}(p_{22} + p_{23}),$$

$$\frac{dy_{14}}{d\tau} = p_{23}y_{13},$$

where $m = 1, \ldots, 4$ and $n = 1, \ldots, 5$.

The initial conditions for Eqs. (A.1) are the following: $y_{0,n}(0) = y_{00,n}$, $y_{1,n}(0) = 0$, $y_{2,n}(0) = 0$, $y_{3,n}(0) = 0$, $y_{4,n}(0) = 0$, $y_{5,n}(0) = 0$, $y_{6,n}(0) = 0$, $y_1(0) = y_{01}$, $y_2(0) = y_{02}$, $y_3(0) = y_{03}$, $y_4(0) = y_{04}$, $y_5(0) = 0$, $y_6(0) = y_{06}$, $y_{7,m}(0) = y_{07,m}$, $y_8(0) = 0$, $y_9(0) = y_{09}$, $y_{10}(0) = 0$, $y_{11}(0) = 0$, $y_{12}(0) = y_{012}$, $y_{13}(0) = 0$, and $y_{14}(0) = 0$, where $m = 1, \ldots, 4$ and $n = 1, \ldots, 5$.

Here $y_{00,n}$, y_{01}, y_{02}, y_{03}, y_{04}, y_{06}, $y_{07,m}$, y_{09}, and y_{012} are the time-independent parameters representing the normalized initial concentrations of mismatches, MutS$_2$, MutL$_2$, MutH, GATCm, UvrD, exonucleases, PolIII, and DNA ligase, respectively. The initial levels of all the intermediate complexes are assumed to be zero at the beginning of repair. The normalization of the variables of the model is performed for the initial concentration of the MutS protein: $y_i = X_i/X_{01}$, and $y_{0i} = X_{0i}/X_{01}$. The values of the parameters X_{0i} for the *in vivo* MMR system are presented in Table B.1.

13

APPENDIX B. PARAMETER VALUES

The dimensionless parameters of Eqs. (A.1) are $\tau = k_{13}t$, $p_1 = k_1 X_{01}/k_{13}$, $p_2 = k_2/k_{13}$, $p_3 = k_3 X_{01}/k_{13}$, $p_4 = k_4/k_{13}$, $p_{5,n} = k_{5,n} X_{01}/k_{13}$, $p_{6,n} = k_{6,n}/k_{13}$, $p_{7,n} = k_{7,n} X_{01}/k_{13}$, $p_{8,n} = k_{8,n}/k_{13}$, $p_{9,n} = k_{9,n}/k_{13}$, $p_{10,n} = k_{10,n} X_{01}/k_{13}$, $p_{11,n} = k_{11,n}/k_{13}$, $p_{12,n} = k_{12,n}/k_{13}$, $p_{13} = k_{13}/k_{13} = 1$, $p_{14} = k_{14} X_{01}/k_{13}$, $p_{15} = k_{15}/k_{13}$, $p_{16} = X_{0L}/\gamma$, $p_{17} = 1/\gamma$, $p_{18} = k_{18}/k_{13}$, $p_{19} = k_{19} X_{01}/k_{13}$, $p_{20} = k_{20}/k_{13}$, $p_{21} = k_{21} X_{01}/k_{13}$, $p_{22} = k_{22}/k_{13}$, and $p_{23} = k_{23}/k_{13}$. Here, t is the dimensional time; k_{13} is the rate constant of non-specific losses of the MMR proteins because of dilution due to bacterial growth; X_{01} is the basal level of the MutS protein in the cell in the absence of MMR-inducing lesions, and γ is the dissociation rate constant of the LexA monomer from the *uvrD* gene operator.

Most of the parameters k_j were determined by fitting the developed model to the *in vitro* experimental data on the MMR kinetics for the ExoI and RecJ pathways [27]. The fitting procedure is performed for a MutH-mediated incision, strand excision by exonucleases, and DNA resynthesis by PolIII. Each of these three stages was investigated for $3'$ and $5'$ DNA nicking. The fitted values for the parameters k_1, k_3, $k_{5,1} = k_{5,2} = k_{5,4}$, $k_{5,3} = k_{5,5}$, $k_{6,1} = k_{6,2} = k_{6,4}$, $k_{6,3} = k_{6,5}$, $k_{7,1} = k_{7,2} = k_{7,4}$, $k_{7,3} = k_{7,5}$, $k_{9,1} = k_{9,2} = k_{9,4}$, $k_{9,3} = k_{9,5}$, $k_{10,1}$, $k_{10,5}$, $k_{12,1}$, $k_{12,5}$, k_{14}, k_{19}, and k_{20} are presented in Table B.1. To obtain these parameters, we have set the initial conditions according to the reactant concentrations for *in vitro* reactions in [27]: $X_{00,1} = 2.4 \cdot 10^{-9}$ M, $X_{00,5} = 2.4 \cdot 10^{-9}$ M, $X_{01} = 3.7 \times 10^{-8}$ M, $X_{02} = 2.5 \cdot 10^{-8}$ M, $X_{03} = 1.0 \cdot 10^{-8}$ M, $X_{06} = 1.2 \cdot 10^{-8}$ M, $X_{07,1} = 1.8 \cdot 10^{-9}$ M, and $X_{07,4} = 7.8 \cdot 10^{-9}$ M. Since the number of GATCm sequences equals the total number of mismatches of all kinds, we set $X_{04} = X_{00,1} + X_{00,2} + X_{00,3} + X_{00,4} + X_{00,5}$. We have set the kinetic rates k_2, k_4, $k_{8,n}$, $k_{11,n}$, k_{13}, k_{15}, k_{18}, and k_{22} equal to zero because the experiment was performed in a constant reaction volume excluding the factor of cell culture growing. In Eqs. (A.1), we have also omitted the following terms corresponding to the synthesis of the MMR proteins: y_{01}, y_{02}, y_{03}, y_{04}, $y_{06}(1 + p_{16})^h / (1 + (p_{17}y_L)^h)$, $y_{07,m}$, y_{09}, and y_{012}.

The parameters $k_{10,2}$, $k_{10,3}$, $k_{10,4}$, $k_{12,2}$, $k_{12,3}$, and $k_{12,4}$ are defined using $k_{10,1}$, $k_{10,5}$, $k_{12,1}$, and $k_{12,5}$ values as well as the relations between the turnover numbers of ExoI, RecJ and ExoVII, and ExoX. The exonuclease turnover numbers were taken from the experimental data: $6.9 \cdot 10^3$ nt/min (nucleotides per minute) for ExoI [28], 10^3 nt/min for RecJ [29], $2.5 \cdot 10^3$ nt/min for ExoVII [30], and $1.4 \cdot 10^3$ nt/min for ExoX [31]. The parameter γ is assumed to be equal to the average value of the LexA dissociation rate from the SOS-box [13, 32]. The value of the Hill coefficient h is defined from the data on the binding cooperativity of the LexA repressor and the *uvrD* regulatory region. As there is the only region of LexA binding to the *uvrD* operator [20], h equals 2, according to Aksenov et al. [23].

Table B.1. Parameters of the model

Parameter	Value	Reference
k_1	$5.2 \cdot 10^7 \ \mathrm{M^{-1} \ min^{-1}}$	This paper
$k_2, k_4, k_{8,n}, k_{11,n}, k_{13}, k_{15}, k_{18}, k_{22}$	$0.0116 \ \mathrm{min^{-1}}$	[23]
k_3	$1.3 \cdot 10^3 \ \mathrm{M^{-1} \ min^{-1}}$	This paper
$k_{5,1}, k_{5,2}, k_{5,4}$	$1.4 \cdot 10^8 \ \mathrm{M^{-1} \ min^{-1}}$	This paper
$k_{5,3}, k_{5,5}$	$1.2 \cdot 10^5 \ \mathrm{M^{-1} \ min^{-1}}$	This paper
$k_{6,1}, k_{6,2}, k_{6,4}$	$0.221 \ \mathrm{min^{-1}}$	This paper
$k_{6,3}, k_{6,5}$	$3.3 \cdot 10^{-4} \ \mathrm{min^{-1}}$	This paper
$k_{7,1}, k_{7,2}, k_{7,4}$	$4.9 \cdot 10^3 \ \mathrm{M^{-1} \ min^{-1}}$	This paper
$k_{7,3}, k_{7,5}$	$3.2 \cdot 10^5 \ \mathrm{M^{-1} \ min^{-1}}$	This paper
$k_{9,n}$	$1.4 \cdot 10^{-4} \ \mathrm{min^{-1}}$	This paper
$k_{10,1}$	$6.7 \cdot 10^4 \ \mathrm{M^{-1} \ min^{-1}}$	This paper
$k_{10,2}$	$2.4 \cdot 10^4 \ \mathrm{M^{-1} \ min^{-1}}$	This paper
$k_{10,3}$	$2.8 \cdot 10^4 \ \mathrm{M^{-1} \ min^{-1}}$	This paper
$k_{10,4}$	$1.4 \cdot 10^4 \ \mathrm{M^{-1} \ min^{-1}}$	This paper
$k_{10,5}$	$1.1 \cdot 10^4 \ \mathrm{M^{-1} \ min^{-1}}$	This paper
$k_{12,1}$	$0.255 \ \mathrm{min^{-1}}$	This paper
$k_{12,2}$	$0.092 \ \mathrm{min^{-1}}$	This paper
$k_{12,3}$	$2.2 \cdot 10^{-4} \ \mathrm{min^{-1}}$	This paper
$k_{12,4}$	$0.052 \ \mathrm{min^{-1}}$	This paper
$k_{12,5}$	$8.7 \cdot 10^{-5} \ \mathrm{min^{-1}}$	This paper
k_{14}	$3.2 \cdot 10^7 \ \mathrm{M^{-1} \ min^{-1}}$	This paper
k_{19}	$3.9 \cdot 10^7 \ \mathrm{M^{-1} \ min^{-1}}$	This paper
k_{20}	$2.9 \ \mathrm{min^{-1}}$	This paper
k_{21}	$1.8 \cdot 10^6 \ \mathrm{M^{-1} \ min^{-1}}$	[35]
k_{23}	$0.021 \ \mathrm{min^{-1}}$	[35]
γ	$1.4 \cdot 10^{-7} \ \mathrm{M}$	[13, 31]
h	2	[23]
X_{0L}	$2.2 \cdot 10^{-6} \ \mathrm{M}$	[36]
X_{01}	$3.1 \cdot 10^{-7} \ \mathrm{M}$	[37]
X_{02}	$1.9 \cdot 10^{-7} \ \mathrm{M}$	[37]
X_{03}	$2.2 \cdot 10^{-7} \ \mathrm{M}$	[37]
X_{06}	$5.0 \cdot 10^{-6} \ \mathrm{M}$	[38]
$X_{07,1}$	$1.5 \cdot 10^{-8} \ \mathrm{M}$	[39]
$X_{07,2}$	$1.1 \cdot 10^{-7} \ \mathrm{M}$	[39]
$X_{07,3}$	$8.9 \cdot 10^{-5} \ \mathrm{M}$	[31]
$X_{07,4}$	$8.3 \cdot 10^{-9} \ \mathrm{M}$	[40]
X_{09}	$5.0 \cdot 10^{-8} \ \mathrm{M}$	[41]
X_{012}	$5.0 \cdot 10^{-7} \ \mathrm{M}$	[42]
$\theta_{0, \ mutS}$	4	[4]
$\theta_{0, \ mutL}$	3.4	[4]
$\theta_{0, \ mutH}$	4.1	[4]
$\theta_{0, \ umu, \ mut}$	2.7	[4]
θ_1	10^{-9}	[33]
θ_2	$3.31 \cdot 10^{-2}$	[34, 23]
$\theta_{3, \ mut+}$	$2.72 \cdot 10^{-9}$	This paper
$\theta_{3, \ mutS}$	$6.95 \cdot 10^{-9}$	This paper
$\theta_{3, \ mutL}$	$4.9 \cdot 10^{-9}$	This paper
$\theta_{3, \ mutH}$	$4.39 \cdot 10^{-9}$	This paper

As it was described earlier [13], the linear component of (3) characterizes the mutagenic lesions, which are fixed during constitutive repair or DNA replication [7]. The mutagenic effectiveness can be defined by the DNA PolIII processing effectiveness. Therefore, according to [33], the coefficient of the linear component can be defined as $\theta_1 = 10^{-9}$. The value of the parameter θ_2, characterizing the number of premutation lesions in an individual gene, is defined as follows. Since we use the *lacZ* gene for the analysis, let $L_1 = 3,075$ base pairs be the length of this gene, $L_0 = 4,639,675$ base pairs be the length of the whole *E. coli's* K-12 MG1655 genome [34], and $m_0 = 50$ J$^{-1} \cdot$ m^2 is the yield of the premutation lesions per full bacterial chromosome [23]. Then the average number of lesions in the *lacZ* gene is $L_1 m_0 \Psi / L_0 = \theta_2 \Psi$. Therefore, the proportionality coefficient is $\theta_2 = L_1 m_0 / L_0 = 3.31 \cdot 10^{-2}$.

Using the MMR model, it is possible to determine the coefficient θ_3 more precisely than in our previous study. The results obtained before indicated an ambiguous and complicated dependence of the resulting mutation frequency on the effectiveness of translesion synthesis. This fact was reflected in our SOS mutagenesis model by introducing the free parameter $P(X)$, describing the probability of wrong nucleotide insertion by the PolV Mut complex, which affects the θ_3 value. According to our previous calculations, $\theta_3 = L_1 k_s / L_0$, where k_s is the slope coefficient of a linear function, which characterises the dependence of the average number of the occurring errors on the UV energy fluence. Simultaneous running of the models for SOS mutagenesis, translesion synthesis, and the MMR system for a mut^+ strain gives $k_s = 4.1 \cdot 10^{-6}$ under $P(X) = 6.1 \cdot 10^{-8}$ and, therefore, $\theta_3 = 2.7 \cdot 10^{-9}$. For the mut^- strains, these values are, respectively, the following: $mutS^-$, $k_s = 1.05 \cdot 10^{-5}$, $P(X) = 1.6 \cdot 10^{-7}$, $\theta_{3,\,mutS} = 6.95 \cdot 10^{-9}$; $mutL^-$, $k_s = 7.4 \cdot 10^{-6}$, $P(X) = 1.1 \cdot 10^{-7}$, $\theta_{3,\,mutL} = 4.9 \cdot 10^{-9}$; $mutH^-$, $k_s = 6.62 \cdot 10^{-6}$, $P(X) = 9.8 \cdot 10^{-8}$, $\theta_{3,\,mutH} = 4.39 \cdot 10^{-9}$.

REFERENCES

1. R. S. Lahue, K. G. Au, P. Modrich, DNA mismatch correction in a defined system, Science 245 (1989) 160–164. doi: 10.1126/science.2665076

2. P. Modrich, R. Lahue, Mismatch repair in replication fidelity, genetic recombination, and cancer biology, Annu. Rev. Biochem. 65 (1996) 101–133. doi: 10.1146/annurev.bi.65.070196.000533

3. G. M. Li, Mechanisms and functions of DNA mismatch repair, Cell Res. 18 (2008) 85–98. doi: 10.1038/cr.2007.115

4. L. Hongbo, R. Stephen, H. B. Hays, J. B. Hays, Antagonism of ultraviolet-light mutagenesis by the methyl-directed mismatch-repair system of Escherichia coli, Genetics 154 (2000) 503–512.

5. L. M. Martinet, B. Marples, M. Coffey, M. Lawler, T. H. Lynch, D. Hollywood, L. Marignol, DNA mismatch repair and the DNA damage response to ionizing radiation: Making sense of apparently conflicting data, Cancer Treat. Rev. 36 (2010) 518–527. doi:10.1016/j.ctrv.2010.03.008

6. M. Radman, Phenomenology of an inducible mutagenic DNA repair pathway in Escherichia coli: SOS-repair hypothesis, in: L. Prakash, F. Sherman, M. Miller, C. Lawrence, H.W. Tabor (Eds.), Molecular and Environmental Aspects of Mutagenesis, Springfield, 1974, pp.128–142.

7. E. M. Witkin, Ultraviolet mutagenesis and inducible DNA repair in Escherichia coli, Bacteriol. Rev. 40 (1976) 869–907.

8. E. A. Krasavin, C. Kozubek, Mutagenic action of radiation with different LET, Energoatomizdat, Moscow, 1991.

9. Z. Wang, Translesion synthesis by the UmuC family of DNA polymerase, Mutat. Res. 486 (2001) 59–70. doi:10.1016/S0921-8777(01)00089-1

10. I. Yang, H. Miller, Z. Wang, E. G. Frank, H. Ohmori, F. Hanaoka, M. Moriya, Mammalian translesion DNA synthesis across an acrolein-derived deoxyguanosine adduct, J. Biol. Chem. 278 (2003) 13989–13994. doi: 10.1074/jbc.M212535200

11. D. Chiapperino, M. Cai, J. M. Sayer, H. Yagi, H. Kroth, C. Masutani, F. Hanaoka, D. M. Jerina, A. M. Cheh, Error-prone translesion synthesis by human DNA polymerase Z on DNA-containing deoxyadenosine adducts of 7,8-dihydroxy-9,10-epoxy-7,8,9,10-tetrahydrobenzo[a]pyrene, J. Biol. Chem. 280 (2005), 39684–39692. doi: 10.1074/jbc.M508008200

12. M. Tang, P. Pham, X. Shen, J. S. Taylor, M. O'Donnell, R. Woodgate, M. F. Goodman, Roles of E. coli DNA polymerases IV and V in lesion-targeted and untargeted SOS mutagenesis, Lett. Nat. 404 (2000) 1014–1018. doi:10.1038/35010020

13. O. V. Belov, E. A. Krasavin, A. Yu. Parkhomenko, Model of SOS-induced mutagenesis in bacteria Escherichia coli under ultraviolet irradiation, J. Theor. Biol. 261 (2009) 388–395. doi:10.1016/j.jtbi.2009.08.016

14. M. Radman, R. Wagner, Mismatch repair in Escherichia coli, Ann. Rev. Genet. 20 (1986) 523–538. doi: 10.1146/annurev.ge.20.120186.002515

15. S. W. Matson, A. B. Robertson, The UvrD helicase and its modulation by the mismatch repair protein MutL. Nucleic Acids Res. 34 (2006) 4089–4097. doi: 10.1093/nar/gkl450

16. B. E. Dutra, V. A. Sutera, J. T. Lovett, S. T. Lovett, RecA-independent recombination is efficient but limited by exonucleases, Proc. Natl. Acad. Sci. USA, 104 (2007) 216–221. doi: 10.1073/pnas.0608293104

17. A. Kornberg, T. A. Baker, DNA replication, W. H. Freeman and Company, New York, 1992.

18. O. V. Belov, E. A. Krasavin, A. Yu. Parkhomenko, SOS response dynamics in Escherichia coli bacterial cells upon ultraviolet irradiation. Physics of Particles and Nuclei Letters 6 (2009) 260–273. doi: 10.1134/S1547477109030121

19. O. V. Belov, E. A. Krasavin, A.Yu. Parkhomenko, Mathematical model of induced mutagenesis in bacteria Escherichia coli under ultraviolet irradiation. Biophysics 55 (2010) 682–690. doi: 10.1134/S0006350910040287

20. A. M. Easton, S. R. Kushner, Transcription of the uvrD gene of Escherichia coli is controlled by the lexA repressor and by attenuation, Nucleic Acids Res. 11 (1983) 8625–8640.

21. J. Courcelle, A. Khodursky, B. Peter, P. O. Brown, P. C. Hanawalt, Comparative gene expression profiles following UV exposure in wild-type and SOS-deficient Escherichia coli, Genetics 158 (2001) 41–64.

22. S. V. Aksenov, E. A. Krasavin, A. A. Litvin, Mathematical model of the SOS response regulation of an excision repair deficient mutant of Escherichia coli after ultraviolet light irradiation, J. Theor. Biol. 186 (1997) 251–260. doi: 10.1006/jtbi.1996.0353

23. S. V. Aksenov, Induction of the SOS Response in ultraviolet-irradiated Escherichia coli analyzed by dynamics of LexA, RecA and SulA proteins, J. Biol. Phys. 25 (1999) 263–277. doi: 10.1023/A:1005163310168

24. Z. Livneh, DNA damage control by novel DNA polymerases: translesion replication and mutagenesis, J. Biol. Chem. 276 (2000) 25639–25642. doi:10.1074/jbc.R100019200

25. V. G. Vaidyanathan, B. P. Cho, Sequence effects on translesion synthesis of an aminofluorene-DNA adduct: conformational, thermodynamic, and primer extension kinetic studies, Biochemistry 51 (2012) 1983–1995. doi: 10.1021/bi2017443

26. J. Malina, O. Novakova, G. Natile, V. Brabec, The thermodynamics of translesion DNA synthesis past major adducts of enantiomeric analogues of antitumor cisplatin, Chem. Asian J. 7 (2012) 1026–1031. doi: 10.1002/asia.201100886

27. A. Pluciennik, V. Burdett, O. Lukianova, M. O'Donnell, P. Modrich, Involvement of the β clamp in methyl-directed mismatch repair in vitro, J. Biol. Chem. 248 (2009) 32782–32791.

28. D. Lu, M. A. Windsor, S. H. Gellman, J. L. Keck, Peptide inhibitors identify roles for SSB C-terminal residues in SSB/Exonuclease I complex formation, Biochemistry 48 (2009) 6764–6771. doi: 10.1021/bi900361r

29. E. S. Han, D. L. Cooper, N. S. Persky, V. A. Sutera, R. D. Whitaker, M. L. Montello, S. T. Lovett, RecJ exonuclease: substrates, products and interaction with SSB, Nucleic Acids Res. 34 (2006) 1084–1091. doi: 10.1093/nar/gkj503

30. A. A. Larrea, I. M. Pedroso, A. Malhotra, R. S. Myers, Identification of two conserved aspartic acid residues required for DNA digestion by a novel thermophilic Exonuclease VII in Thermotoga maritima, Nucl. Acids Res. 36 (2008) 5992–6003. doi: 10.1093/nar/gkn588

31. M. Viswanathan, S. T. Lovett, Exonuclease X of Escherichia coli. A novel 3ʹ-5ʹ DNase and DnaQ superfamily member involved in DNA repair, J. Biol. Chem. 274 (1999) 30094–30100. doi: 10.1074/jbc.274.42.30094

32. R. Mohana-Borges, A. B. F. Pacheco, F. J. R. Sousa, D. Foguel, D. F. Almeida, J. L. Silva, LexA repressor forms stable dimers in solution, J. Biol. Chem. 275 (2000) 4708–4712. doi:10.1074/jbc.275.7.4708

33. J. W. Drake, Spontaneous Mutation: Comparative Rates of Spontaneous Mutation, Nature 221 (1969) 1132. doi: 10.1038/2211133a0

34. I. M. Keseler, J. Collado-Vides, A. Santos-Zavaleta, M. Peralta-Gil, S. Gama-Castro, L. Muñiz-Rascado, C. Bonavides-Martinez, S. Paley, M. Krummenacker, T. Altman, P. Kaipa, A. Spaulding, J. Pacheco, M. Latendresse, C. Fulcher, M. Sarker, A. G. Shearer, A. Mackie, I. Paulsen, R. P. Gunsalus, P. D. Karp, EcoCyc: a comprehensive database of Escherichia coli biology, Nucleic Acids Res. 39 (2011) D583–D590. doi: 10.1093/nar/gkq1143

35. D. Georlette, Z. O. Jonsson, F. Van Petegem, J.-P. Chessa, J. Van Beeumen, U. Hubscher, C. Gerday, A DNA ligase from the psychrophile Pseudoalteromonas haloplanktis gives insights into the adaptation of proteins to low temperatures, Eur. J. Biochem. 267 (2000) 3502–3512. doi: 10.1046/j.1432-1327.2000.01377.x

36. S. Hegde, S. J. Sandler, A. J. Clark, M. V. Madiraju, recO and recR mutations delay induction of the SOS response in Escherichia coli, Mol. Gen. Genet. 246 (1995) 254–258. doi: 10.1007/BF00294689

37. G. Feng, H. C. Tsui, M. E. Winkler, Depletion of the cellular amounts of the MutS and MutH methyl-directed mismatch repair proteins in stationary-phase Escherichia coli K-12 cells, J. Bacteriol. 178 (1996) 2388–2396.

38. M. A. Petit, E. Dervyn, M. Rose, K. D. Entian, S. McGovern, S. D. Ehrlich, C. Bruand, PcrA is an essential DNA helicase of Bacillus subtilis fulfilling functions both in repair and rolling-circle replication, Mol. Microbiol. 29 (1998) 261–273. doi: 10.1046/j.1365-2958.1998.00927.x

39. D. L. Cooper, R. S. Lahue, P. Modrich, Methyl-directed mismatch repair is bidirectional, J. Biol. Chem. 268 (1993) 11823–11829.

40. T. J. Haggerty, S. T. Lovett, IF3-Mediated Suppression of a GUA Initiation Codon Mutation in the recJ Gene of Escherichia coli, J. Bacteriol. 179 (1997) 6705–6713.

41. C. S. McHenry, A. Kornberg, DNA polymerase III holoenzyme of Escherichia coli, Purification and resolution into subunits, J. Biol. Chem. 252 (1977) 6478–6484.

42. E. C. Friedberg, G. C. Walker, W. Siede, DNA repair and mutagenesis, ASM Press, Washington, D.C., 1995.

Редактор *С. В. Савиных*